

Electronic structure, Mechanical and Thermodynamic properties of CoYSb (Y= Cr, Mo, W) half-Heusler compounds as potential spintronic materials

O. T. Uto

Federal University of Agriculture

J. O. Akinlami

Federal University of Agriculture

S. Kenmoe (✉ stephane.kenmoe@uni-due.de)

University of Duisburg-Essen

G. A. Adebayo

Federal University of Agriculture

Research Article

Keywords: nearly half-metal, Spin-polarization, Poisson's ratio, thermodynamic properties, Electronic band Structure

Posted Date: November 5th, 2021

DOI: <https://doi.org/10.21203/rs.3.rs-1033376/v1>

License: © ⓘ This work is licensed under a Creative Commons Attribution 4.0 International License.

[Read Full License](#)

Electronic structure, Mechanical and Thermodynamic properties of CoYSb (Y= Cr, Mo, W) half-Heusler compounds as potential spintronic materials

O. T. Uto^{a,1}, J. O. Akinlami^a, S. Kenmoe^{b,1} and G. A. Adebayo^{a,1}

^a*Department of Physics, Federal University of Agriculture, P.M.B. 2240, Abeokuta, Nigeria*

^b*Department of Theoretical Chemistry, University of Duisburg-Essen, Universitätsstr. 2, D-45141 Essen, Germany*

Abstract

The CoYSb (Y = Cr, Mo and W) compounds which are XYZ type half-Heusler alloys and also exist in the face centred cubic MgAgAs-type structure conform to $F\bar{4}3m$ space group. In the present work, these compounds are investigated in different atomic arrangements called, Type-I, Type-II and Type-III phases, using Generalized Gradient Approximation (GGA) in the Density Functional Theory (DFT) implemented in QE (Quantum Espresso *Ab-Initio* Simulation Package). The ferromagnetic state of these alloys is studied after investigating their stable structural phase. The calculated electronic band structure and the total electronic density of state indicated nearly half-metallic behaviour in CoMoSb with a possibility of being used in spintronic application, metallic in CoWSb and half-metallic in CoCrSb, with the minority-spin band gap of 0.81 eV. Furthermore, the calculated mechanical properties predicted an anisotropic behaviour of these alloys in the stable phase. Finally, due to its high Debye temperature value, CoCrSb possesses a stronger covalent bond than CoMoSb and CoWSb, respectively.

Keywords: nearly half-metal, Spin-polarization, Poisson's ratio, thermodynamic properties, Electronic band Structure

¹authors to whom correspondence can also be sent: uto@physics.unaab.edu.ng, stephane.kenmoe@uni-due.de and adebayo@physics.unaab.edu.ng

1. Introduction

Ternary half-Heusler (HH) compounds involving Co atom have recently attracted attention due to their high curie temperature, and structural similarity with binary semiconductors with zinc-blende (ZB) structure that makes them potential candidates in optoelectronic and spintronic applications such as quantum sensors, resistors and computers devices, respectively in the near future [1]-[4], topological insulator [5]-[6], and thermoelectric devices [7], [14]. The wide range of usage of HH in applications is due to its excellent electrical, mechanical and electronic properties and thermal stability. The crystal structure, $C1_b$, of any HH alloy is similar to the structure, $L2_1$, of a full-Heusler alloy (X_2YZ) but missing one X atom. The absence of inversion symmetry due to an empty X site and the low coordination number of the d-band metals in the HH alloys are believed to be essential for these materials novel electronic and magnetic properties. Some research groups have reported three possible distinct atomic arrangements, called Type-I, Type-II, and Type-III phases, due to this missing X atom in the HH alloy [1], [8]-[18]. In Table 1, the positions occupied by the atoms and the vacancy are given according to the notations defined by Wyckoff [19]. Researchers such as [12]-[18], [7] have theoretically predicted and reported some Co-based HH compounds using Density Functional Theory in which they reported it to be semiconductor, metallic and half-metallic depending on the valence electron count (VEC) of the alloys. In the interest to study the structural, mechanical and thermodynamics properties of such predicted compounds, CoYSb (Y=Cr, Mo, W) compound has been chosen. To the best of our knowledge, we report here, for the first time, its band structure, mechanical and thermodynamics properties to explore their electronic transport behaviour and chemical bonding between their atoms. In Section 2, we explain a brief description of the computational details used. Then, in Section 3, the structural and magnetic properties for each phase of ferromagnetic HH CoYSb (Y=Cr, Mo, W) at its optimized lattice constant and the influence of the lattice parameter will be presented on the magnetic properties for each phase discussed. Next, in Section 4, the electronic properties of the stable phase showing both spin band and spin DOS will be presented and discussed. Also, the mechanical properties of the stable phase ferromagnetic HH CoYSb (Y=Cr, Mo, W) will be reported in Section 5. Finally, in Section 6, thermodynamic properties with summarising of our results in conclusion. To the extent we know, these detailed calculations have not been done before for all series of CoYSb alloys

38 considered in this work.

39 2. computational details

40 All computations have been performed using the Quantum Espresso *Ab-*
41 *Initio* simulation package, which is a first-principles plane-wave pseudopo-
42 tential [21]-[23] to study the electronic and magnetic properties of CoYSb
43 (Y=Cr, Mo, W) in the three phases mentioned above. The generalized gra-
44 dient approximation (GGA) was used in treating the effects of exchange-
45 correlation potential with Perdew-Burke-Ernzerhof parameterization (PBE)
46 [24]. The cutoff wave function was set at 680 eV, and the k-point of $14 \times$
47 14×14 Monkhorst-Pack meshes [27] grid was used in the irreducible Brillouin
48 zone to calculate the total charge density. The Plane-waves pseudopotential
49 (PWPP) basis functions set consists of the $3d^7 4s^2$, $3d^5 4s^1$, $4d^5 5s^1$, and $5d^7$
50 $6s^2$ for Co, Cr, Mo and W respectively, as well as $5s^2 5p^3$ for Sb elements with
51 a self-consistent convergence total energy of less than 10^{-4} Ry. Thermo_pw
52 code [25], [26] was used to obtain the mechanical and thermodynamic proper-
53 ties based on our optimized lattice constant and cutoffs wave functions with
54 denser k-points to get an accurate result.

55 3. Structural and Magnetic Properties

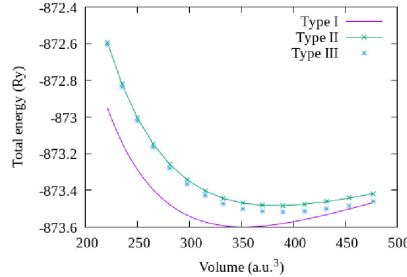
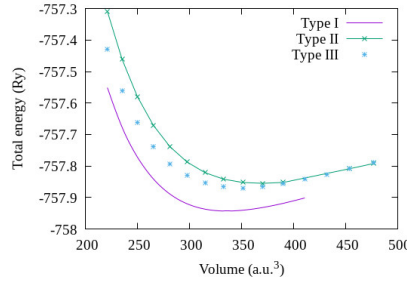
56 Firstly, we investigated the equilibrium lattice constant of the HH com-
57 pound CoYSb (Cr, Mo, W) based on the three possible arrangement that
58 was reported by researchers on the site preference of X and Y atoms which
59 affects the properties of HH due to the high influence of the d elements and
60 the position of the sp-valent element as shown on the Wyckoff positions of
61 the atoms in Table 1.

Table 1: The Wyckoff positions of the three atoms, X, Y, and Z: $4a = (0, 0, 0) a$, $4b = (0.5, 0.5, 0.5) a$ and $4c = (0.25, 0.25, 0.25) a$, with the 4d site vacant

Structural phase	X	Y	Z
Type I	4c	4b	4a
Type II	4b	4a	4c
Type III	4a	4c	4b

62 The optimized structural parameters of these alloys in each phase, en-
63 ergy–volume graphics of these systems were plotted by fitting to Murnaghan

64 equation of states [20] to obtain the equilibrium lattice constant (a_o), bulk
 65 modulus (B), the minimum energy (E_{min}) and pressure derivative (B') of our
 66 alloys been studied in Type-I, Type-II and Type-III phases which conforms
 67 to $F\bar{4}3m$ space group as reported in Table 2. The minimum energy obtained
 68 from the fitted energy–volume curves of CoYSb (Y = Cr, Mo, W) alloys
 69 shows that the most stable and suitable phase is the Type-I phase, as shown
 70 in Fig.1. The lattice parameters are the smallest in the Type-I phase; Bulk
 71 moduli are more significant in the Type-I phase than the other structural
 72 phases. Also, they have large pressure derivatives of bulk moduli, which in-
 73 dicates that these alloys display strong sensitivity against pressure change in
 74 all structural phases. Type-I CoYSb alloys are the more stable phase, and
 75 hence, we shall focus our attention more on the study of this phase. Firstly,
 76 we investigated the equilibrium lattice constant of the HH compound CoYSb
 77 (Cr, Mo, W) based on the three possible arrangement that was reported by
 78 researchers on the site preference of X and Y atoms which affects the prop-
 79 erties of HH due to the strong influence of the d elements and the position
 80 of the sp-valent element as shown on the Wyckoff positions of the atoms in
 81 Table 1.



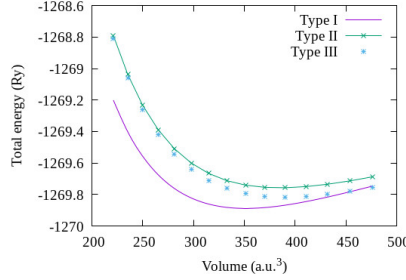


Figure 1: Calculated total energy as a function of volume in ferromagnetic state for the three possible structural phase for CoCrSb, CoMoSb and CoWSb respectively.

Table 2: The optimized lattice constants, a_o (\AA), equilibrium energies, E_{min} (Ry), bulk modulus, B (GPa) and pressure derivative for the bulk modulus, B' for CoYSb (Y= Cr, Mo, W) for the three possible structural phases by Murnaghan equation of state.

Alloys	Calculations	Structural phase	a_o (\AA)	B (GPa)	B'	E_{min} (Ry)
CoCrSb	This work	Type I	5.848	121.4	4.66	-757.944
		other calculations	5.79 ^a			
			5.820 ^b	135.4 ^b		
			5.800 ^c			
			Type II	6.031	97.6	4.33
		Type III	5.935	98.6	4.71	-757.869
			5.935 ^d			
CoMoSb	other calculations	Type I	5.937	152.2	4.62	-873.598
			5.935 ^d			
		Type II	6.134	124.1	4.13	-873.484
		Type III	6.140	131.6	3.94	-873.520
CoWSb		Type I	5.939	164.9	4.32	-1269.888
		Type II	6.133	138.7	4.01	-1269.758
		Type III	6.145	148.2	3.81	-1269.819

a Ref.[14]

b Ref.[15]

c Ref.[16]

d Ref.[13]

82 The calculated total and partial magnetic moments for all phases are
83 listed in Table 3., It is seen from the table that the main contribution to the

84 total magnetic moment for these alloys comes from the Y atom for CoCrSb
 85 and Co-atom for the Type-II and Type-III of CoYSb (Y= Mo, W). Since
 86 the total magnetic moment in CoYSb (Y = Cr, Mo and W) for the phases
 87 are greater than 1, it can be said that these materials show ferromagnetic
 88 properties. Hence, Type-I CoCrSb alloy exhibit a half-metallic behaviour,
 89 and its probably due to its small Y radius, which correlates with a decrease
 90 in its lattice parameter compared to CoMoSb and CoWSb, which have a
 91 larger lattice constant because Mo 4d and W 5d states have a smaller width
 92 relative to that of the Cr 3d state. So the oversized Co atom is effectively
 93 due to the enormously widened lattice because of the large Mo and W atoms.
 94 This possibly is the reason for the large change in the total magnetic moment
 95 compared with that of an integer number of Cr atom. Many half-Heusler
 96 alloys follow the Slater-Pauling (SP) rule $M_t = Z_t - 18$ [28], [29] where Z_t
 97 is the total number of the valence electron and 18 means that there are 9
 98 occupied spin-down states per unit cell. Thus CoMoSb and CoWSb, just like
 99 CoCrSb alloy has a total 20 valence electron count and should have a total
 100 magnetic moment of $2 \mu_B$ that does not agree with the result obtained.

Table 3: The calculated spin magnetic moments in μ_B for CoYSb (Y=Cr, Mo, W) compounds for the three possible structural phases comparing with available data.

$m^{spin}(\mu_B)$	Calculations	Structural phase	Co	Y	Sb	Void	Total
CoCrSb	This work	Type I	-0.4473	2.3766	-0.0573	0.138	2.01
		other calculations	-0.36 ^a	2.37 ^a	-0.06 ^a		2.00 ^a
		Type II	-0.4917	3.0659	-0.0625	0.328	2.84
		Type III	1.1219	1.8089	-0.0177	0.01169	3.03
CoMoSb		Type I	0.6685	0.9017	-0.0148	0.2346	1.79
		Type II	1.0329	0.4100	0.0136	0.0435	1.20
		Type III	0.9274	0.0711	0.0297	0.0082	1.02
	other calculations		0.650 ^b	1.111 ^b	-0.037 ^b		1.82 ^b
CoWSb		Type I	1.0274	1.2957	-0.0285	0.1955	2.49
		Type II	0.8804	0.1896	-0.0178	0.0078	1.06
		Type III	1.6376	0.4698	0.0133	0.0293	2.15

a Ref.[16]

b Ref.[13]

101 Our calculated values show slight deviation from other theoretical values
 102 available obtained by us for Type-I CoCrSb and CoMoSb [16], [13] with a

103 minimal discrepancy of only less than 1 % and suggesting that our compu-
 104 tational method is reasonable and agreed with the available data.

105 4. Electronic band structure

106 The band structures calculation of the minority-spin states, which lies
 107 within the semiconductor region and the majority states been metallic, was
 108 performed to analyze the half-metallic nature of these materials. These spin-
 109 polarized band calculations for Type-I CoYSb (Y= Cr, Mo, W) was carried
 110 out at equilibrium lattice constant in the ferromagnetic state along the high
 111 symmetry directions in the first Brillouin zone are shown in Fig. 2, in which
 112 the majority-spin band channels energy bands exhibit a metallic overlap with
 113 the E_F with their minority-spin band channel semiconductors the maximum
 114 of valence band occurs at the Γ -point and conduction band minimum is at
 115 the X-point, resulting in a band gap of 0.81 eV for CoCrSb half-Heusler
 116 alloy is slightly higher than the previous calculated value 0.77 eV, but the
 117 half-metallic gap is in good comparison with the previous calculation [16].
 118 The minority-spin states gap of CoCrSb is also predicted for CoMoSb and
 119 CoWSb, respectively. But these gaps apparently becomes broader, and the
 120 Fermi level is pushed further away from the gap but closer to the conduction
 121 bands of the minority-spin electrons with the maximum valence band occurs
 122 at the L-point and conduction band minimum is at the X-point, which leads
 123 to a band gap of 0.32 eV for CoMoSb has seen in Fig. 3, which apparently
 124 distort the half-metallic property of these alloys. These distortions in the
 125 band gap width are found to be dependent on the lattice parameters and the
 126 atomic radius of the substitute Y element.

Table 4: The calculated minority-spin band gap, half-metallic (HM) gap and % spin polarization (SP) of Type I CoYSb (Y= Cr, Mo, W).

Compound	Calculations	Band gap (eV)	HM gap (ev)	SP %
CoCrSb	This work	0.81	0.21	100
	others	0.77 ^a	0.22 ^a	
CoMoSb		0.32		72
	others			23 ^b
CoWSb				33

a Ref.[16]

b Ref.[13]

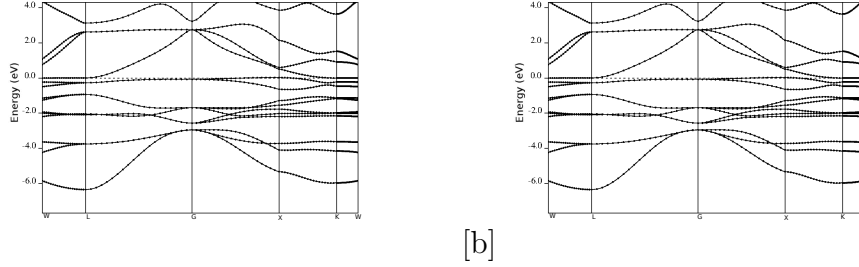


Figure 2: Band structures for CoCrSb (a) majority-spin and (b) minority-spin. The Fermi level is indicated by the dashed horizontal line.

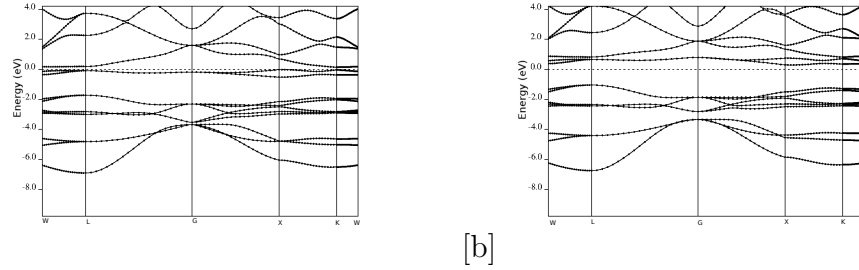


Figure 3: Band structures for CoMoSb (a) majority-spin and (b) minority-spin. The Fermi level is indicated by the dashed horizontal line.

127 To further confirm the possible half-metallicity of CoYSb (Y = Cr, Mo,
 128 W), we show in Fig.4 the calculated total spin density of state (TDOS) for
 129 CoCrSb, CoMoSb and CoWSb, respectively in the Type-I arrangement. It
 130 can be seen that all these mentioned alloys show various degrees of half-
 131 metallic behaviours: in the majority-spin (up spin) channel, whose energy
 132 bands exhibit a metallic overlap with the E_F , whereas in the minority-spin
 133 (down spin) direction, an energy gap is opened and the E_F locates within the
 134 gap for CoCrSb and slightly close to the conduction band for CoMoSb and
 135 into the conduction band for CoWSb. This is seen from the spin polarization
 136 calculation in which it decreases from 100 % for CoCrSb to 33 % for CoWSb
 137 as shown in table 4., which is estimated by using the spin polarization (P)
 138 at the Fermi energy (E_F) following the expression:

$$P = \frac{n \uparrow (E_F) - n \downarrow (E_F)}{n \uparrow (E_F) + n \downarrow (E_F)} \times 100\% \quad (1)$$

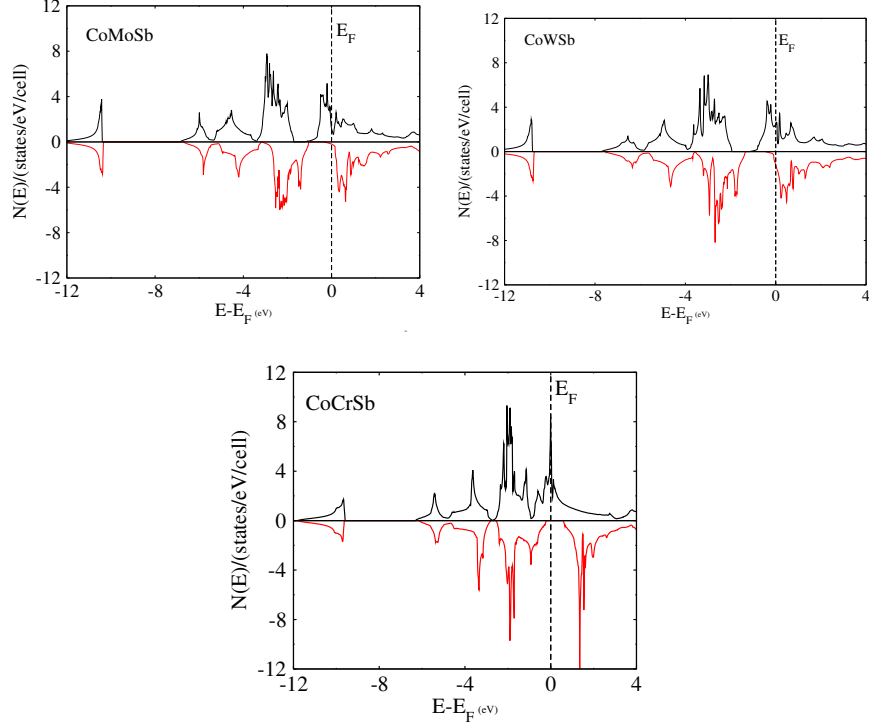


Figure 4: Calculated total spin density of states (DOS) of Type-I CoYSb alloy.

139 5. Mechanical Properties

140 In this section, we discuss the mechanical properties and phase stability.
 141 The stable structure (Type-I) mechanical properties, such as the elastic constants
 142 for a cubic structure which are reduced into Three independent elastic
 143 constants C_{11} , C_{12} , and C_{44} , respectively. The link between mechanical and
 144 dynamic behaviour of a material such as shear modulus (G), bulk modulus
 145 (B), and young modulus (E) is usually obtained through the stress-strain
 146 method [30]. First, we test the mechanical stability of these compounds based
 147 on the durability of the crystal against external forces, which is a desirable
 148 property to ensure its sustainability in any application. The mechanical stability
 149 according to the Born and Huang stability criteria for cubic structure
 150 [32]

$$C_{11} > 0, C_{44} > 0, C_{11} - C_{12} > 0, \text{ and } C_{11} + 2C_{12} > 0. \quad (2)$$

151 The calculated elastic values for the stable structures CoYSb ($Y=Cr$,

152 MO, and W) satisfy the above stability criteria. Hence, these compounds
 153 are mechanically stable, as shown by our results in Table 5. Furthermore,
 154 using the Voigt-Reuss-Hill approximation [33]-[34] which estimate the shear
 155 modulus (G), bulk modulus (B), Poisson's ratio (ν), and Young modulus (E)
 156 were calculated by using the following equations:

$$G = \frac{C_{11} + 2C_{12}}{3} \quad (3)$$

$$B = \frac{C_{11} - C_{12} + 3C_{44}}{5} \quad (4)$$

$$\nu = \frac{3B - 2G}{2(3B + G)} \quad (5)$$

$$E = \frac{9BG}{3B + G} \quad (6)$$

157 The shear anisotropy (A), The Pugh's [31] ratio and the inverse which is
 158 Frantsevich's ratio given by the expression

$$A = \frac{2C_{44}}{C_{11} - C_{12}} \quad (7)$$

159 The bulk (B) and shear (G) are important in alloy applications due to
 160 the empirical rule, in which materials with high B and G tend to have a high
 161 melting point and high Debye temperature. Generally, B and G show how
 162 resistive these alloys are when subjected to fracture and plastic deformation,
 163 respectively. The higher the value B, the more its resistance to deformation
 164 due to pressure. CoWSb resistance to pressure is stronger compared
 165 to CoMoSb and CoCrSb, as shown in Table 5. The value of shear mod-
 166 ulus G shows the resistance of a material to deformation by shear stress.
 167 The higher the value G, the higher its resistance to shear stress. Hence,
 168 CoCrSb > CoMoSb > CoWsb. The Young's modulus E characterizes the ma-
 169 terial's stiffness, and the higher the value E, the stiffer is the material. There-
 170 fore, as shown in Table 5, the relative order of stiffness, CoCrSb, is stiffer
 171 than CoMoSb, and CoWSb is the least stiffer. Also, the unidirectional elastic
 172 constant C_{11} is much higher than that of C_{44} indicating that these compounds
 173 present weaker resistance to pure shear deformation compared to resistance
 174 to unidirectional compression.

Table 5: Various mechanical properties of CoYSb (Y= Cr, Mo, W) stable phase obtained from the calculated lattice.

Calculated properties	CoCrSb	CoMoSb	CoWSb
C_{11} (GPa)	202.83	250.02	264.14
C_{12} (GPa)	79.61	117.98	131.46
C_{44} (GPa)	55.11	42.30	30.16
$C_{11}-C_{12}$ (GPa)	123.22	132.04	123.68
$C_{11} + 2C_{12}$ (GPa)	362.04	485.97	527.05
B (GPa)	120.66	161.99	175.68
G (GPa)	57.63	50.59	41.61
E (GPa)	149.19	137.45	115.64
A	0.49	0.64	0.45
ν	0.29	0.36	0.39
Pugh's ratio	2.09	3.20	4.22

175 We also deduced the cubic Shear anisotropy factor [37] for these com-
176 pounds based on equation 7. The calculated result shows anisotropy fac-
177 tors as 0.49, 0.64 and 0.45 for CoCrSb, CoMoSb and CoWSb, respectively.
178 From these values, one can deduce that these compounds are substantially
179 anisotropic in nature. The degree of ductility of a material is explained by
180 the Pugh ratio, which is the ratio of the bulk and shear modulus of the ma-
181 terial. The material is said to be more ductile if the Pugh's ratio increase
182 more and it is greater than 1.75 ($G/B < 0.57$) [38], otherwise it is brittle.
183 As shown in Table 5, we can see that the compounds are ductile in nature
184 because their values are greater than 1.75. The Poisson's ratio (ν) charac-
185 terises the bonding forces in material and its compression against external
186 forces [39]-[40]. The alloys reported in this work are central-force solid (ν is
187 generally between 0.25 to 0.5) and incompressible because ν is due to their
188 values that lie within this range. Hence, indicating that the metallic bonding
189 contribution to the atomic bond is dominant.

190 6. Thermodynamic Properties

191 The effects of temperature at constant pressure on the thermodynamic
192 properties of the CoYSb (Y= Cr, Mo, W) material from the state equation,
193 under the considerations of the quasi-harmonic approximation of the Debye
194 model, were analyzed as presented below. Fig. 5 shows the results of specific

195 heat at constant volume, C_V , as functions of temperature. As can be seen in
 196 the figure, the temperature was varied between 0 K and 800 K at constant
 197 pressure.

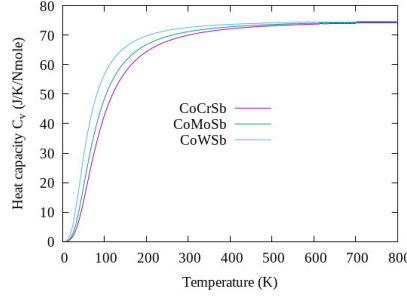


Figure 5: Heat capacity C_v against temperature for Type-I CoYSb alloy

198 Fig. 5 shows more clearly the trend of specific heat towards the Dulong-
 199 Petit limit, which is the specific heat value independent of temperature. From
 200 this limit value of Dulong-Petit, as the temperature increases, each of the
 201 atoms in the material absorbs the same amount of energy proportional to
 202 this temperature increase. This value corresponds to 72.63 J/Nmol.K for
 203 CoCrSb and CoMoSb respectively while 73.47 J/Nmol.K for CoWSb. The
 204 Debye temperature is a fundamental parameter of thermodynamic, which
 205 is linked with many physical properties of the material such as the melt-
 206 ing temperature, lattice vibrations and specific heat at low temperature[41].
 207 These properties listed in table 6 were obtained from the calculated elastic
 208 constants using the following equations.

$$v_l = \sqrt{\frac{3B + 4G}{3\rho}} \quad (8)$$

$$v_s = \sqrt{\frac{G}{\rho}} \quad (9)$$

209 Where, (v_l) is the compressional velocity and shear sound velocity (v_s).
 210 The average sound velocity (v_m) is expressed in terms of compressional and
 211 shear sound velocities as stated below.

$$v_m = \left(\frac{1}{3}\right)^{1/3} \left[\frac{2}{v_s^3} + \frac{1}{v_l^3} \right] \quad (10)$$

212 The Debye temperature θ_D is thus expressed as

$$\theta_D = \frac{\hbar}{\kappa} \left(\frac{3n}{4\pi} \left(\frac{\rho N_A}{M} \right) \right)^{1/3} v_m \quad (11)$$

213 Where, \hbar is the reduced Planck's constant, κ is Boltzmann's constant, N_A is
 214 Avogadro's number, M is atomic mass of unit cell, n is the number of atomic
 215 per formula unit, and ρ is the density.

Table 6: Average sound velocity (v_m), compressional velocity (v_l), shear sound velocity (v_s), Debye temperature (θ_D) and predicted melting temperature (T_m) for the stable phase CoYSb (Y= Cr, Mo, W).

Compound	v_l (m/s)	v_s (m/s)	v_m (m/s)	θ_D (K)	T_m (K)
CoCrSb	5027.79	2723.03	3037.67	354.68	1751.73±300
CoMoSb	5105.36	2397.30	2688.55	308.93	2030.62±300
CoWSb	4459.49	1891.93	2113.76	243.05	2114.07±300

216 The Covalence bonds strength in solids is characterized by Debye tem-
 217 perature, which is listed in the table above along with the predicted melting
 218 temperature estimated from our elastic constant C_{11} calculated using the
 219 following expression [42].

$$T_{(melting)} = [555K + \left(\frac{5.91K}{GPa} \right) C_{11} \pm 300K] \quad (12)$$

220 Hence, CoCrSb has a stronger bond than CoMoSb and CoWSb due to
 221 its high Debye temperature.

222 6.1. Conclusions

223 The structural, mechanical, electronic and thermodynamic properties of
 224 Co-based half-Heusler CoYSb (Y= Cr, Mo, W) alloys which conform to
 225 $F\bar{4}3m$ space group in the three possible structural (Type-I, Type-II and
 226 Type-III) phases atomic arrangements, which are given by Wyckoff notation
 227 have been investigated in detail. We determined that our alloys are stable
 228 in the Type-I structural phase, which is half-metallic for CoCrSb, nearly
 229 half-metallic for CoMoSb due to its percentage spin polarization with the
 230 possibility of being used in a spintronic application and metallic character
 231 for CoWSb due to the absence of band gaps in their spin-polarized electronic

232 band structures. The calculated electronic band structures and total mag-
233 netic moments show that these alloys are ferromagnetic in all the phases.
234 Finally, some mechanical properties of these materials have been examined
235 in the most stable phase (Type-I), and it is clearly seen that these alloys are
236 stable mechanically and anisotropic in nature.

237 **References**

- 238 [1] D. Kieven, R. Klenk, S. Naghavi, C. Felser, and T. Gruhn, Phys. Rev. B
239 81, 075208 (2010).
- 240 [2] S. Wurmehl, G. H. Fecher, H. C. Kandpal, V. Kseno-fontov, C. Felser,
241 H. J. Lin and J. Morais, Phys. Rev. B 72, 184434 (2005).
- 242 [3] S. A. Wolf, D. D.Awschalom, R. A.Buhrman, J. M.Daughton, S.von Mol-
243 nar, M. L.Roukes, A. Y. Chtchelkanova and D. M. Treger, Science 294:
244 1488-1495 16 NOVEMBER 2001.
- 245 [4] A. Roy, J. W. Bennett, K. M. Rabe, and D. Vanderbilt, Phys. Rev. Lett.
246 109, 037602 (2012).
- 247 [5] D. Xiao, Y. Yao, W. Feng, J. Wen, W. Zhu, X.Q. Chen, G.M. Stocks,
248 and Z. Zhang, Phys. Rev. Lett. 105 (2010), p. 096404.
- 249 [6] H. Lin, L.A. Wray, Y. Xia, S. Xu, S. Jia, R.J. Cava, A. Bansil, and M.Z.
250 Hasan, Nat. Mater. 9 (2010), pp. 546–549.
- 251 [7] M. Zeeshan, H.K. Singh, J. Van den Brink and H. C. Kandpal, Phys.
252 Rev. Mater. 1 (2017) 075407.
- 253 [8] S. D Li, Z. R Yuan, L.Y. Lu, M.M. Liu, Z.G. Huang, F. M Zhang, Y.W.
254 Du, Mater. Sci. Eng., A 428 (2006) 332.
- 255 [9] P. Larson, S. D. Mahanti, and M. G. Kanatzidis, Phys. Rev.B 62, 12754
256 (2000).
- 257 [10] F. B. Mancoff, J. F. Bobo, O. E. Richter, K. Bessho, P. R. Johnson,
258 R. Sinclair, W. D. Nix, R. White, and B. M. Clemens, J. Mater. Res. 14,
259 1560 (1999).
- 260 [11] R. A. de Groot, F. M. Mueller, P. G. van Engen, and K. H. J. Buschow,
261 Phys. Rev. Lett. 50, 2024 (1983).

- 262 [12] I. Galanakis, P. Mavropoulos, and P. H. Dederichs, *J. Phys. D* 39, 765
263 (2006).
- 264 [13] B.R.K. Nanda, J. I Dasgupta, *Phys. Condens. Matter* 15 (2003)
265 73077323.
- 266 [14] S. Minami, I. Fumiyuki, M. P. Yo and S. Mineo, *AIP: Applied Physics*
267 *Letter* 113, 032403.
- 268 [15] H.C.Kanpal, C. Felse and R. Seshadri, *J. of phys. D: App. Phys.* 39,
269 776.
- 270 [16] Y.Zhong-Yu, S. Li, P. Meng-Mei and S. Shu-Juan, *Acta Phys. Sin.* Vol.
271 65, No. 12 (2016) 127501.
- 272 [17] J. Tobola and J. Pierre, *J. Alloys Compd.* 296, 243 (2000).
- 273 [18] S. E Kulkova, S. V Eremeev, T. Kakeshita, S. S Kulkov and G. E Ruden-
274 ski, *mater. Trans.* Vol 47, No 3 (2006) 604.
- 275 [19] R. W. G. Wyckoff, *Crystal Structures*, 2nd ed., Vol. 1 (John Wiley and
276 Sons, 1963).
- 277 [20] F. D. Murnaghan, *Proc. Natl. Acad. Sci. USA.* 30 (1944) 244.
- 278 [21] S. Scandolo, P. Giannozzi, C. Cavaoni, S. de Gironcoli, A. Pasquarello
279 and S. Baroni, *Z. Kristallogr.* 220 (2005) 574579.
- 280 [22] P. Giannozzi, S. Baroni, N. Bonini, M. Calandra, R. Car, C. Cavazzoni,
281 D. Ceresoli, G. L. Chiarotti, M. Cococcioni, I. Dabo, A. D. Corso, S. de
282 Gironcoli, S. Fabris, G. Fratesi, R. Gebauer, U. Gerstmann, C. Gougoussis,
283 A. Kokalj, M. Lazzeri, L. Martin-Samos, N. Marzari, F. Mauri, R. Maz-
284 zarello, S. Paolini, A. Pasquarello, L. Paulatto, C. Sbraccia, S. Scandolo,
285 G. Sciauzero, A. P. Seitsonen, A. Smogunov, P. Umari, R. M. Wentzcov-
286 itch, *J. Phys.:Condens. Matter* 21 (39) (2009) 395502.
- 287 [23] P. Giannozzi, O. Andreussi, T. Brumme, O. Bunau, M. Buongiorno
288 Nardelli, M. Calandra, R. Car, C. Cavazzoni, D. Ceresoli, M. Cococcioni,
289 N. Colonna, I. Carnimeo, A. Dal Corso, S. de Gironcoli, P. Delugas, R. A.
290 DiStasio Jr, A. Ferreti, A. Floris, G. Fratesi, G. Fugallo, R. Gebauer, U.
291 Gerstmann, C. Gougoussis, F. Giustino, T. Gorni, J. Jia, M. Kawamura,

- 292 H. Y Ko, A. Kokalj, E. Kkbenli, M. Lazzeri, M. Marsili, N. Marzari, F.
293 Mauri, N. L. Nguyen, H. V. Nguyen, A. Otero-de-la-Roza, L. Paulatto, S.
294 Ponc, D. Rocca, R. Sabatini, B. Santra, M. Schlipf, A. P. Seitsonen, A.
295 Smogunov, I. Timrov, T. Thonhauser, P. Umari, N. Vast, X. Wu and S.
296 Baroni. 2017 *J. Phys.: Condens. Matter* 29 465901.
- 297 [24] J. P. Perdew, K. Burke, and M. Ernzerhof, *Phys. Rev. Lett.* 77 (1996)
298 3865.
- 299 [25] <https://dalcorso.github.io/thermopw>
- 300 [26] A. Dal Corso, *J. of Phys.: Condens. Matter* 28 (2016) 075401.
- 301 [27] H. J. Monkhorst and J. D. Pack, *Phys. Rev. B* 13 (1976) 5188.
- 302 [28] J. Kubler, *Phys. B+C* 127 (1984) 257.
- 303 [29] I. Galanakis, P. H Dederichs and P. H Mavropoulos: *Phys. Rev. B* 66
304 (2002) 174429.
- 305 [30] Y. Le Page and P. Saxe, *Phys. Rev. B.* 65 (2002) 104104.
- 306 [31] S. F. Pugh, *Philos. Mag.* 45 (1954) 823.
- 307 [32] M. Born and K. Huang, *Dynamical Theory of Crystal Lattices* (Oxford:
308 Oxford Clarendon Press, 1956), pp 120-156.
- 309 [33] W. Voigt, *Lehrbuck der Kristallphysik* (B. B. Teubner, Leipzig, 1928),
310 pp 739.
- 311 [34] H. B. Huntington, *Solid State Physics*, F. Seitz and D. Properties of En-
312 gineering Ceramics, W. Kriegel and H. Palmour, Turnbull, Eds. (Academic
313 Press Inc., New York, 1958), Vol. 7
- 314 [35] A. Reuss, *Z. Angew. Math. Mech.* 9 (1929) 49.
- 315 [36] R. Hill, *Proc. Phys. Soc. (London)* 65 (1952) 349.
- 316 [37] C. Zener, *Elasticity and Anelasticity of Metals*, University of Chicago
317 Press, Chicago, 1948.
- 318 [38] A. R. Degheidy, E. B. Elkenany, *Chin. Phys.* 26 (2017) 086103.

- 319 [39] D. C. Gupta and S. Ghosh, *J. Magn. Magn. Mater.* 435 (2017), pp.
320 107-116.
- 321 [40] H. Fu, D. Li, F. Peng, T. Gao, and X. Cheng, *Comput. Mater. Sci.* 44
322 (2008), pp. 774-778.
- 323 [41] O.L. Anderson, *J. Phys. Chem. Solids* 24 (1963) 909.
- 324 [42] M.E. Fine, L.D. Brown, and H.L. Marcus, *Scr. Metall.* 18 (1984), pp.
325 951-956